Warm and dense stellar matter under strong magnetic fields

A. Rabhi,[1,2] P. K. Panda,[3,1] and C. Providência[1]

[1]*Centro de Física Computacional, Department of Physics, University of Coimbra, P-3004-516 Coimbra, Portugal*

[2]*Laboratoire de Physique de la Matiére Condensée, Faculté des Sciences de Tunis, Campus Universitaire, Le Belvédére-1060, Tunisia*

[3]*Department of Physics, C.V. Raman College of Engineering, Vidya Nagar, Bhubaneswar-752054, India*

(Received 27 April 2011; revised manuscript received 9 July 2011; published 8 September 2011)

We investigate the effects of strong magnetic fields on the equation of state of warm stellar matter as it may occur in a protoneutron star. Both neutrino-free and neutrino-trapped matter at a fixed entropy per baryon are analyzed. A relativistic mean-field nuclear model, including the possibility of hyperon formation, is considered. A density-dependent magnetic field with a magnitude of 10^{15} G at the surface and not more than 3×10^{18} G at the center is considered. The magnetic field gives rise to a neutrino suppression, mainly at low densities, in matter with trapped neutrinos. It is shown that a hybrid protoneutron star will not evolve into a low-mass black hole if the magnetic field is strong enough and the magnetic field does not decay. However, the decay of the magnetic field after cooling may give rise to the formation of a low-mass black hole.

DOI: 10.1103/PhysRevC.84.035803 PACS number(s): 21.65.−f, 97.60.Jd, 26.60.−c, 95.30.Tg

I. INTRODUCTION

Neutron stars with very strong magnetic fields are known as magnetars [1–3]. Recent observations suggest that anomalous x-ray pulsars and soft γ-ray repeaters are candidates for magnetars [4–6]. The magnetic field at the surface of the magnetars may be as strong as 10^{14}–10^{15} G, and magnetars are warm young stars ∼1-kyear old. On the other hand, it is estimated that the interior field in neutron stars may be as large as 10^{18} G [7]. Ferrario and Wickammasinghe [8] suggest that the extra strong magnetic field of the magnetars results from their stellar progenitor with a high magnetic-field core. Iwazaki [9] proposed that the huge magnetic field of the magnetars is some color ferromagnetism of quark matter. Recently, Vink and Kuiper [10] have suggested that the magnetars originate from rapid rotating protoneutron stars.

Motivated by the existence of strong magnetic fields in neutron stars, theoretical studies on the effects of extremely large fields on dense matter and neutron stars have been carried out by many authors [11–18]. For densities below twice normal nuclear-matter density ($\rho \sim 0.153$ fm^{-3}), the matter only consists of nucleons and leptons. However, for baryon densities above $2\rho_0$, the equation of state (EOS) and the composition of matter is much less certain, and the strangeness degrees of freedom should be taken into account through the inclusion of hyperons, kaon condensation, or a deconfinement phase transition into strange quark matter. The inclusion of hyperons and pion or kaon condensation in stars with strong magnetic fields [19–25] tends to soften the EOS at high densities.

In Ref. [19], it was shown that the threshold densities of hyperons can significantly be altered by strong magnetic fields. Similar conclusions were obtained in Ref. [23] where the strangeness was included through an antikaon condensation or in Ref. [24] where not only hyperons, but also the strange mesons σ^* and ϕ were included in the EOS.

The effects of the magnetic field on the structure and composition of a neutron star that allows quark-hadron phase transition has been studied in Ref. [26]. A strong magnetic field makes the overall EOS softer. However, due to the positive contribution of the magnetic-field pressure to the total EOS, an increase in the maximum mass is predicted [19,25,27,28]. Also, the effects of the magnetic field on quark matter [28–34] and on the color superconducting phases of dense matter, which could exist in the core of compact stars, have been investigated extensively [35–40].

Protoneutron stars appear as the outcome of the gravitational collapse of a massive star. During its early evolution, the protoneutron star, with an entropy per baryon on the order of 1 (units of the Boltzmann constant), contains trapped neutrinos. This stage is followed by a deleptonization period, during which the core is heated up and reaches an entropy per particle $\mathfrak{s} \sim 2$, before cooling occurs. During the cooling stage, exotic degrees of freedom, such as hyperons or a kaon condensate, will appear [41].

In this paper, we focus on the properties of warm stellar matter under a strong magnetic field, which is composed of a chemically equilibrated and charge-neutral mixture of nucleons, hyperons, and leptons. We will consider both neutrino-free matter and matter with trapped neutrinos. The effect of the magnetic field on the composition of warm stellar matter, both with trapped neutrinos and neutrino free, and the properties of the EOS will be discussed. Both the Landau quantization, which affects the charged particles and the incorporation of the nucleon anomalous magnetic moments (AMMs) for field strengths $B > 10^5 B_e^c$ ($B_e^c = 4.414 \times 10^{13}$ G is the electron critical field) have important effects.

This paper is organized as follows: In Sec. II, we derive the EOS for hadronic matter at finite temperatures with a magnetic field. We present the results in Sec. III. Finally, the conclusions are summarized in Sec. IV.

II. HADRON-MATTER EOS

For the description of the EOS of stellar matter, we employ a field-theoretical approach in which the baryons interact via the exchange of σ-ω-ρ mesons in the presence of a static magnetic field B along the z axis [42–44].

The Lagrangian density of the nonlinear Walecka model that we consider has the form [43]

$$\mathcal{L} = \sum_b \mathcal{L}_b + \mathcal{L}_m + \sum_l \mathcal{L}_l. \tag{1}$$

The baryon, lepton ($l = e, \mu$), and meson (σ, ω, and ρ) Lagrangians are given by [42,44]

$$\begin{aligned}
\mathcal{L}_b &= \bar{\Psi}_b\big(i\gamma_\mu\partial^\mu - q_b\gamma_\mu A^\mu - m_b + g_{\sigma b}\sigma - g_{\omega b}\gamma_\mu\omega^\mu \\
&\quad - g_{\rho b}\tau_{3_b}\gamma_\mu\rho^\mu - \tfrac{1}{2}\mu_N\kappa_b\sigma_{\mu\nu}F^{\mu\nu}\big)\Psi_b, \\
\mathcal{L}_l &= \bar{\psi}_l(i\gamma_\mu\partial^\mu - q_l\gamma_\mu A^\mu - m_l)\psi_l, \\
\mathcal{L}_m &= \tfrac{1}{2}\partial_\mu\sigma\,\partial^\mu\sigma - \tfrac{1}{2}m_\sigma^2\sigma^2 - U(\sigma) + \tfrac{1}{2}m_\omega^2\omega_\mu\omega^\mu \\
&\quad - \tfrac{1}{4}\Omega^{\mu\nu}\Omega_{\mu\nu} - \tfrac{1}{4}F^{\mu\nu}F_{\mu\nu} + \tfrac{1}{2}m_\rho^2\boldsymbol{\rho}_\mu\boldsymbol{\rho}^\mu - \tfrac{1}{4}\mathbf{R}^{\mu\nu}\mathbf{R}_{\mu\nu},
\end{aligned} \tag{2}$$

where Ψ_b and ψ_l are the baryon and lepton Dirac fields, respectively. The index b runs over the eight lightest baryons n, p, Λ, Σ^-, Σ^0, Σ^+, Ξ^-, and Ξ^0, and the sum on l is over electrons and muons (e^- and μ^-). σ, ω, and ρ represent the scalar, the vector, and the vector-isovector meson fields, which describe the nuclear interaction, and $A^\mu = (0, 0, Bx, 0)$ refers to an external magnetic field along the z axis. The baryon mass and isospin projection are denoted by m_b and τ_{3_b}, respectively. The mesonic and electromagnetic-field tensors are given by their usual expressions: $\Omega_{\mu\nu} = \partial_\mu\omega_\nu - \partial_\nu\omega_\mu$, $\mathbf{R}_{\mu\nu} = \partial_\mu\boldsymbol{\rho}_\nu - \partial_\nu\boldsymbol{\rho}_\mu$, and $F_{\mu\nu} = \partial_\mu A_\nu - \partial_\nu A_\mu$. The baryon AMMs are introduced via the coupling of the baryons to the electromagnetic-field tensor with $\sigma_{\mu\nu} = \frac{i}{2}[\gamma_\mu, \gamma_\nu]$ and strength $\kappa_b = (\mu_b/\mu_N - q_b m_p/m_b)\mu_N$, where μ_N is the nucleon magneton and μ_b, q_b, and m_b, respectively, are the magnetic moment, the charge, and the mass of baryon b. The values of κ_b used in the present paper were taken from Ref. [19]. The electromagnetic field is assumed to be generated externally (and, thus, has no associated field equation), and only frozen-field configurations are considered. The interaction couplings are denoted by g, the electromagnetic couplings are denoted by q, and the baryon, meson, and lepton masses are denoted by m. The scalar self-interaction is taken to be of the form

$$U(\sigma) = \tfrac{1}{3}bm_n(g_{\sigma N}\sigma)^3 + \tfrac{1}{4}c(g_{\sigma N}\sigma)^4. \tag{3}$$

From the Lagrangian density in Eq. (1), we obtain the following meson-field equations in the mean-field approximation:

$$m_\sigma^2\sigma + \frac{\partial U(\sigma)}{\partial\sigma} = \sum_b g_{\sigma b}\rho_b^s = g_{\sigma N}\sum_b x_{\sigma b}\rho_b^s, \tag{4}$$

$$m_\omega^2\omega^0 = \sum_b g_{\omega b}\rho_b^v = g_{\omega N}\sum_b x_{\omega b}\rho_b^v, \tag{5}$$

$$m_\rho^2\rho^0 = \sum_b g_{\rho b}\tau_{3_b}\rho_b^v = g_{\rho N}\sum_b x_{\rho b}\tau_{3_b}\rho_b^v, \tag{6}$$

where $\sigma = \langle\sigma\rangle$, $\omega^0 = \langle\omega^0\rangle$, and $\rho = \langle\rho^0\rangle$ are the nonvanishing expectation values of the meson fields in uniform matter, and ρ_b^v and ρ_b^s, respectively, are the baryon vector and scalar densities.

The Dirac equations for baryons and leptons, respectively, are given by

$$\begin{aligned}
&\big[i\gamma_\mu\partial^\mu - q_b\gamma_\mu A^\mu - m_b^* - \gamma_0(g_\omega\omega^0 + g_\rho\tau_{3_b}\rho^0) \\
&\quad - \tfrac{1}{2}\mu_N\kappa_b\sigma_{\mu\nu}F^{\mu\nu}\big]\Psi_b = 0,
\end{aligned} \tag{7}$$

$$(i\gamma_\mu\partial^\mu - q_l\gamma_\mu A^\mu - m_l)\psi_l = 0, \tag{8}$$

where the effective baryon masses are given by

$$m_b^* = m_b - g_\sigma\sigma, \tag{9}$$

and ρ_b^s and ρ_b^v are the scalar density and the vector density, respectively. For a stellar matter consisting of a β-equilibrium mixture of baryons and leptons, the following equilibrium conditions must be imposed:

$$\mu_b = q_b\mu_n - q_l\mu_e, \tag{10}$$

$$\mu_\mu = \mu_e, \tag{11}$$

where μ_i is the chemical potential of species i ($i = b$ for baryons, $i = n$ for neutrons, $i = e$ for electrons, and $i = \mu$ for muons). The electric-charge neutrality condition is expressed by

$$\sum_b q_b\rho_b^v + \sum_l q_l\rho_l^v = 0, \tag{12}$$

where ρ_i^v is the number density of particle i ($i = b$ for baryons and $i = l$ for leptons). If trapped neutrinos are included, we replace $\mu_e \to \mu_e - \mu_{\nu_e}$ in the above equations,

$$\mu_b = q_b\mu_n - q_l(\mu_e - \mu_{\nu_e}). \tag{13}$$

$$\mu_\mu - \mu_{\nu_\mu} = \mu_e - \mu_{\nu_e}, \tag{14}$$

where μ_{ν_e} and μ_{ν_μ} are the electron and muon neutrino-chemical potentials, respectively. The introduction of additional variables, the neutrino-chemical potentials, requires additional constraints, which we supply by fixing the lepton fraction $Y_{\mathrm{Le}} = Y_e + Y_{\nu_e} = 0.4$ [41,45]. Since no muons are present before and during the supernova explosion, the constraint $Y_{L\mu} = Y_\mu + Y_{\nu_\mu} = 0$ must be imposed. However, because the muon fraction is very small in matter with trapped neutrinos, we only include muons in neutrino-free matter.

The energy spectra for charged baryons, neutral baryons, and leptons (electrons and muons), respectively, are given by

$$E_{\nu,s}^b = \tilde{\varepsilon}_{\nu,s}^b + g_{\omega b}\omega^0 + \tau_{3_b}g_{\rho b}\rho^0, \tag{15}$$

$$E_s^b = \tilde{\varepsilon}_s^b + g_{\omega b}\omega^0 + \tau_{3_b}g_{\rho b}\rho^0, \tag{16}$$

$$E_{\nu,s}^l = \tilde{\varepsilon}_{\nu,s}^l = \sqrt{(k_\parallel^l)^2 + m_l^2 + 2\nu|q_l|B}, \tag{17}$$

where

$$\tilde{\varepsilon}_{\nu,s}^b = \sqrt{(k_\parallel^b)^2 + \left(\sqrt{m_b^{*2} + 2\nu|q_b|B} - s\mu_N\kappa_b B\right)^2}, \tag{18}$$

$$\tilde{\varepsilon}_s^b = \sqrt{(k_\parallel^b)^2 + \left[\sqrt{m_b^{*2} + (k_\perp^b)^2} - s\mu_N\kappa_b B\right]^2}, \tag{19}$$

and $\nu = n + \frac{1}{2} - \mathrm{sgn}(q)\frac{s}{2} = 0, 1, 2, \ldots$ enumerates the Landau levels (LLs) of the fermions with electric charge q, the quantum number s is $+1$ for spin-up and -1 for spin-down cases, and $k_\parallel$, $k_\perp$, respectively, are the momentum components parallel and perpendicular to the magnetic field.

At finite temperature, the occupation-number distribution functions are given for charged and neutral baryons, respectively, by

$$\begin{aligned} f^b_{k,\nu,s} &= \frac{1}{1+\exp\left[\beta\left(\tilde{\varepsilon}^b_{\nu,s}-\mu^*_b\right)\right]}, \\ \bar{f}^b_{k,\nu,s} &= \frac{1}{1+\exp\left[\beta\left(\tilde{\varepsilon}^b_{\nu,s}+\mu^*_b\right)\right]}, \end{aligned} \tag{20}$$

$$\begin{aligned} f^b_{k,s} &= \frac{1}{1+\exp\left[\beta\left(\tilde{\varepsilon}^b_{s}-\mu^*_b\right)\right]}, \\ \bar{f}^b_{k,s} &= \frac{1}{1+\exp\left[\beta\left(\tilde{\varepsilon}^b_{s}+\mu^*_b\right)\right]}, \end{aligned} \tag{21}$$

and for the charged leptons,

$$\begin{aligned} f^l_{k,\nu,s} &= \frac{1}{1+\exp\left[\beta\left(\tilde{\varepsilon}^l_{\nu,s}-\mu_l\right)\right]}, \\ \bar{f}^l_{k,\nu,s} &= \frac{1}{1+\exp\left[\beta\left(\tilde{\varepsilon}^l_{\nu,s}+\mu_l\right)\right]}, \end{aligned} \tag{22}$$

where the baryon-effective chemical potential $(\mu_b)^*$ is given by

$$\mu^*_b = \mu_b - g_{\omega b}\omega^0 - g_{\rho b}\tau_{3_b}\rho^0. \tag{23}$$

For the charged baryons, the scalar and vector densities, respectively, are given by

$$\begin{aligned} \rho^s_b &= \frac{|q_b|Bm^*_b}{2\pi^2}\sum_{\nu,s}\int_0^\infty \frac{dk^b_\parallel}{\sqrt{(k^b_\parallel)^2+\left(\bar{m}^c_b\right)^2}}\left(f^b_{k,\nu,s}+\bar{f}^b_{k,\nu,s}\right), \\ \rho^v_b &= \frac{|q_b|B}{2\pi^2}\sum_{\nu,s}\int_0^\infty dk^b_\parallel\left(f^b_{k,\nu,s}-\bar{f}^b_{k,\nu,s}\right), \end{aligned} \tag{24}$$

where we have introduced the effective mass,

$$\bar{m}^c_b = \sqrt{m^{*2}_b + 2\nu|q_b|B} - s\mu_N\kappa_b B. \tag{25}$$

For the neutral baryons, the scalar and vector densities, respectively, of the neutral baryon b are given by

$$\begin{aligned} \rho^s_b &= \frac{1}{2\pi^2}\sum_s\int_0^\infty k^b_\perp dk^b_\perp\left(1-\frac{s\mu_N\kappa_b B}{\sqrt{m^{*2}_b+(k^b_\perp)^2}}\right) \\ &\quad\times\int_0^\infty dk^b_\parallel\frac{m^*_b}{\tilde{\varepsilon}^b_s}\left(f^b_{k,s}+\bar{f}^b_{k,s}\right), \\ \rho^v_b &= \frac{1}{2\pi^2}\sum_s\int_0^\infty k^b_\perp dk^b_\perp\int_0^\infty dk^b_\parallel\left(f^b_{k,s}-\bar{f}^b_{k,s}\right). \end{aligned} \tag{26}$$

The vector density of the charged leptons is given by

$$\rho^v_l = \frac{|q_l|B}{2\pi^2}\sum_{\nu,s}\int_0^\infty dk^l_\parallel\left(f^l_{k,\nu,s}-\bar{f}^l_{k,\nu,s}\right), \tag{27}$$

and for neutrinos, the vector density is given by

$$\rho^v_{\nu_e} = \frac{1}{2\pi^2}\int_0^\infty k^2 dk\left(f^\nu_{k,s}-\bar{f}^\nu_{k,s}\right). \tag{28}$$

We solve the coupled Eqs. (4)–(8) self-consistently at a given baryon density $\rho=\sum_b\rho^v_b$ in the presence of a strong magnetic field. The energy density of stellar matter is given by

$$\varepsilon_m = \sum_b\varepsilon_b + \sum_{l=e,\mu}\varepsilon_l + \frac{1}{2}m^2_\sigma\sigma^2 + U(\sigma) + \frac{1}{2}m^2_\omega\omega^2_0 + \frac{1}{2}m^2_\rho\rho^2_0, \tag{29}$$

where the energy densities of charged baryons ε^c_b, neutral baryons ε^n_b, and leptons ε_l, respectively, have the following forms:

$$\begin{aligned} \varepsilon^c_b &= \frac{|q_b|B}{2\pi^2}\sum_{\nu,s}\int_0^\infty dk^b_\parallel\sqrt{(k^b_\parallel)^2+\left(\bar{m}^c_b\right)^2}\left(f^b_{k,\nu,s}+\bar{f}^b_{k,\nu,s}\right), \\ \varepsilon^n_b &= \frac{1}{2\pi^2}\sum_s\int_0^\infty k^b_\perp dk^b_\perp\int_0^\infty dk^b_\parallel \\ &\quad\times\sqrt{(k^b_\parallel)^2+\left[\sqrt{m^{*2}_b+(k^b_\perp)^2}-s\mu_N\kappa_b B\right]^2}\left(f^b_{k,s}+\bar{f}^b_{k,s}\right), \\ \varepsilon_l &= \frac{|q_l|B}{2\pi^2}\sum_{\nu,s}\int_0^\infty dk^l_\parallel\sqrt{(k^l_\parallel)^2+m^2_l+2\nu|q_l|B} \\ &\quad\times\left(f^l_{k,\nu,s}+\bar{f}^l_{k,\nu,s}\right). \end{aligned} \tag{30}$$

The thermodynamical grand potential and the free-energy density are defined as

$$\Omega = \mathcal{F} - \sum_b\mu_b\rho^v_b, \quad \mathcal{F} = \varepsilon_m - T\mathcal{S}, \tag{31}$$

where the entropy density $\mathcal{S}$ is given by

$$\mathcal{S} = \sum_b\mathcal{S}_b + \sum_l\mathcal{S}_l, \tag{32}$$

with

$$\begin{aligned} \mathcal{S}^c_b &= -\frac{|q_b|B}{2\pi^2}\sum_{\nu,s}\int_0^\infty dk^b_\parallel\left\{f^b_{k,\nu,s}\ln f^b_{k,\nu,s}+\left(1-f^b_{k,\nu,s}\right)\right. \\ &\quad\times\ln\left(1-f^b_{k,\nu,s}\right)+\bar{f}^b_{k,\nu,s}\ln\bar{f}^b_{k,\nu,s} \\ &\quad\left.+\left(1-\bar{f}^b_{k,\nu,s}\right)\ln\left(1-\bar{f}^b_{k,\nu,s}\right)\right\}, \\ \mathcal{S}^n_b &= -\frac{1}{2\pi^2}\sum_s\int_0^\infty k^b_\perp dk^b_\perp\int_0^\infty dk^b_\parallel\left\{f^b_{k,s}\ln f^b_{k,s}\right. \\ &\quad+\left(1-f^b_{k,s}\right)\ln\left(1-f^b_{k,s}\right) \\ &\quad\left.+\bar{f}^b_{k,s}\ln\bar{f}^b_{k,s}+\left(1-\bar{f}^b_{k,s}\right)\ln\left(1-\bar{f}^b_{k,s}\right)\right\}, \\ \mathcal{S}_l &= -\frac{|q_l|B}{2\pi^2}\sum_{\nu,s}\int_0^\infty dk^l_\parallel\left\{f^l_{k,\nu,s}\ln f^l_{k,\nu,s}+\left(1-f^l_{k,\nu,s}\right)\right. \\ &\quad\times\ln\left(1-f^l_{k,\nu,s}\right)+\bar{f}^\nu_{k,\nu,s}\ln\bar{f}^\nu_{k,\nu,s} \\ &\quad\left.+\left(1-\bar{f}^\nu_{k,\nu,s}\right)\ln\left(1-\bar{f}^\nu_{k,\nu,s}\right)\right\}. \end{aligned} \tag{33}$$

The pressure of neutron-star matter is given by

$$P_m = -\Omega = \mu_n\sum_b\rho^v_b - \varepsilon_m + T\mathcal{S}, \tag{34}$$

where the charge neutrality and β-equilibrium conditions are used to get the last equality. If the stellar matter contains

TABLE I. The parameter set GM1 [43] used in the calculation.

ρ_0 (fm^{-3})	$-B/A$ (MeV)	M^*/M	$g_{\sigma N}/m_\sigma$ (fm)	$g_{\omega N}/m_\omega$ (fm)	$g_{\rho N}/m_\rho$ (fm)	$x_{\sigma H}$	$x_{\omega H}$	$x_{\rho H}$	b	c
0.153	16.30	0.70	3.434	2.674	2.100	0.600	0.653	0.600	0.002 947	−0.001 070

trapped neutrinos, their energy density, pressure, and entropy contributions, respectively,

$$\varepsilon_{\nu_e} = \frac{1}{2\pi^2}\int_0^\infty k^3 dk\{f^\nu_{k,s} + \bar{f}^\nu_{k,s}\},$$
$$P_{\nu_e} = \frac{1}{6\pi^2}\int_0^\infty k^3 dk\{f^\nu_{k,s} + \bar{f}^\nu_{k,s}\},$$
$$\mathcal{S}^{\nu_e}_l = -\frac{1}{2\pi^2}\int_0^\infty (k^l)^2 dk^l\{f^\nu_{k,s}\ln f^\nu_{k,s} + (1-f^\nu_{k,s}) \times \ln(1-f^\nu_{k,s}) + \bar{f}^\nu_{k,s}\ln \bar{f}^\nu_{k,s} + (1-\bar{f}^\nu_{k,s})\ln(1-\bar{f}^\nu_{k,s})\} \quad (35)$$

should be added to the stellar-matter energy and pressure.

III. RESULTS AND DISCUSSION

We now study stellar matter at finite temperatures with magnetic fields. We include the baryonic octet in the EOS and choose the GM1 parameter set [43] for our calculation. The static properties of the baryons were given in previous papers [11,25]. The parameters of the model are the nucleon mass $m_n = 939$ MeV, the masses of mesons m_σ, m_ω, m_ρ, and the coupling constants. The meson-hyperon couplings are assumed to be fixed fractions of the meson-nucleon couplings $g_{iH} = x_{iH} g_{iN}$, where, for each meson i, the values of x_{iH} are assumed equal for all hyperons H. The values of x_{iH} are chosen to reproduce the binding energy of Λ at nuclear saturation as suggested in Ref. [43] and given in Table I. A different choice could have been made to consider that the optical potential of Σ^- in nuclear matter is repulsive as shown in Ref. [46]. However, there is very little experimental information that can be used to fix the Σ^- interaction. Moreover, the main difference that would occur would be the onset of Σ^- at larger densities and Ξ^- at lower densities.

We consider that the external magnetic field is constant. The magnetic field will be defined in units of the critical field $B_e^c = 4.414 \times 10^{13}$ G so that $B = B^* B_e^c$.

In Figs. 1 and 2, the pressure is plotted versus the density for $B^* = 0$, 10^5, and 2×10^5 for neutrino-free matter (Fig. 1) and matter with trapped neutrinos (Fig. 2), without and with the inclusion of the AMMs, respectively, in the left and right panels. We consider an entropy per baryon $\mathfrak{s} = 0$ and 2. The kink on each EOS curve identifies the onset of hyperons. The effects of the AMMs are only noticeable for a strong magnetic field above $B^* = 10^5$ as already discussed in Ref. [11].

We start by discussing neutrino-free matter, which is shown in Fig. 1. The strong magnetic field makes the EOS softer at low densities because of the Landau quantization of charged-particle orbitals and the high degeneracy of these levels [11,25]. The density of baryons per level is proportional to the strength of the magnetic field, and therefore, the stronger the magnetic field, the larger the softening induced by Landau quantization. At low densities, the only baryons affected by the Landau quantization are the protons. Landau quantization reduces the Fermi momentum of protons, and as a result, the equilibrium state has a larger (smaller) fraction of protons (neutrons). Although charge neutrality implies a larger fraction of electrons, these also suffer Landau quantization, and the overall effect is the softening of the EOS. At low densities, if the field is strong enough, all the protons will be in the lowest LL; still, at high densities, more than one LL could be occupied, according to the field intensity. Consequently, the effects of Landau quantization are stronger at low densities than at high densities. The main effects are a softening of the EOS, see the dashed and dotted thin lines in the left panel of Fig. 1 below $2\rho/\rho_0$, and an increase in the proton fraction.

On the other hand, the onset of hyperons occurs at larger densities in the presence of a strong magnetic field, and therefore, the EOS becomes harder at high densities as the thin lines in the left panel of Fig. 1 show above $2\rho/\rho_0$. At finite temperatures, these effects are partially washed out because all levels have a finite probability of being occupied. In the left panel of Fig. 1, it is seen that the EOS for $B^* = 2 \times 10^5$ (dotted thick line) is not much softer than the corresponding EOS for $B^* = 0$ below $2\rho/\rho_0$. Also, a smaller effect is seen at large densities: The EOS does not become so hard above $2\rho/\rho_0$ because of the earlier onset of strangeness at finite temperatures.

The effects of temperature are even stronger when the AMMs are included (right panel). As discussed in Ref. [11], in the presence of a strong magnetic field, the extra hardness

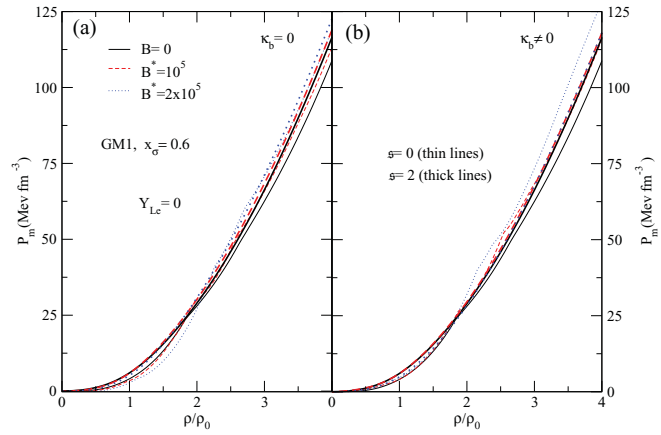

FIG. 1. (Color online) Matter pressure as a function of the baryonic density for several values of a magnetic field ($B^* = 0$, $B^* = 10^5$, 2×10^5) without (left panels) and with AMMs (right panels) for an entropy per baryon $\mathfrak{s} = 0$ and 2 and for neutrino-free matter.

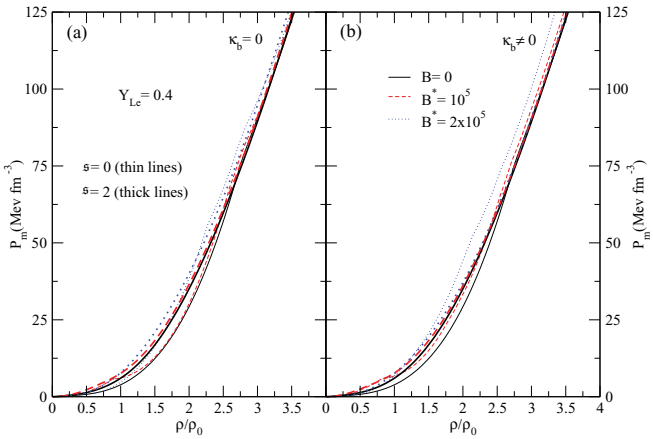

FIG. 2. (Color online) The same as Fig. 1 but for matter with trapped neutrinos and lepton fraction $Y_{\rm Le} = 0.4$.

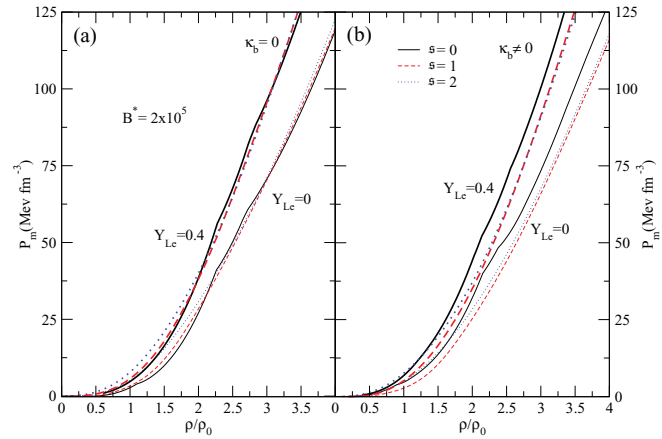

FIG. 3. (Color online) Matter pressure as a function of the baryonic density for $B^* = 2 \times 10^5$: comparison between both neutrino-free and neutrino-trapped matter for several values of the entropy per baryon $\mathfrak{s}$.

obtained with the inclusion of the AMMs is mainly caused by an increase in the neutron-degeneracy pressure because of the spin polarization of the neutrons. In fact, including AMMs induces spin polarization, which increases with increasing B, and a larger polarized neutron fraction gives rise to a larger neutron degeneracy pressure. Temperature partially destroys this degeneracy because there is a finite probability that unoccupied levels at zero temperature become partially occupied and, consequently, give rise to a softening of the EOS: At large densities, the three EOS plotted for $\mathfrak{s} = 2$ with $B^* = 0$, 10^5, and 2×10^5 almost coincide. Whereas, for the zero-magnetic field, the EOS becomes harder with the inclusion of temperature, this is not necessarily true for a strong magnetic field because of the competing effects of temperature and magnetic field.

We conclude that one of the main effects of temperature on the EOS of matter under a strong magnetic field is to wash out the effects of the Landau quantization and spin polarization and to bring the EOS closer to the no-field case. For a strong magnetic field, the temperature will soften the EOS, contrary to what happens for $B = 0$.

In Fig. 2, we show results for matter with trapped neutrinos and a lepton fraction $Y_{\rm Le} = 0.4$. In this case, at low densities, the EOS becomes harder in the presence of a strong magnetic field. This is mainly caused by the larger electron fraction below the onset of strangeness. However, just as before, the effect of the field is not so strong for a finite entropy per baryon. Above $\rho = 2\rho_0$, the equation becomes softer in the presence of a magnetic field both taking into account AMMs or not if $\mathfrak{s} = 2$, although for $\mathfrak{s} = 0$, the opposite occurs. In fact, above this density, for $B^* = 2 \times 10^5$, the proton fraction becomes comparable or even larger than the neutron fraction, and therefore, the kinetic contribution to the pressure reduces. When the AMMs are included, there is not much difference at $\mathfrak{s} = 2$, however, for $\mathfrak{s} = 0$, the EOS is slightly harder than in the case without the AMMs because of a larger electron fraction and a smaller hyperon fraction.

In Fig. 3, to compare the effect of temperature on neutrino-free matter and matter with trapped neutrinos in the presence of a magnetic field, we have plotted, for $B^* = 2 \times 10^5$ and $\mathfrak{s} = 0$, 1, and 2, the pressure for neutrino-free matter and neutrino-trapped matter without (left panel) and with (right panel) AMMs.

At zero-magnetic field, the EOS of matter with trapped neutrinos becomes softer at finite temperatures at low densities [41]. Trapped neutrinos increase (decrease) the proton (neutron) fraction at low density, and this softens the EOS relative to the neutrino-free case because of an overall smaller baryonic kinetic pressure. However, at larger densities, trapped neutrinos hinder the onset of hyperons, therefore, shifting the softening of the EOS caused by strangeness to larger densities [41,47,48]. For $B^* = 2 \times 10^5$ and zero temperature, neutrino-trapped matter is not softer than neutrino-free matter because the decrease in the neutron fraction caused by trapped neutrinos is much smaller, and the overall decrease in the baryonic kinetic pressure does not compensate the increase in the total lepton contribution to the EOS. At finite temperatures, however, the onset of hyperons and leveling out of the neutron and proton fractions at lower densities gives rise to a softening of the EOS for densities $2\rho_0 < \rho < 3\rho_0$.

As discussed before, the inclusion of the AMMs makes the EOS harder, however, finite temperatures wash LL-filling effects and spin-polarization effects, and a softer EOS results.

The behavior of the EOS is determined by the onset of hyperons, the proton-to-neutron ratio and the lepton fraction. In the following, we will analyze how the temperature, in conjunction with a strong magnetic field, affects the particle fractions. In Fig. 4, the particle fraction $Y_i = \rho_i/\rho$ for baryons and leptons is plotted as a function of the baryon density for $B^* = 2 \times 10^5$ (thick lines) and $B^* = 0$ (thin lines) for an entropy per particle $\mathfrak{s} = 0$, 1 and 2. Neutrino-free matter is represented in the left panels, and matter with trapped neutrinos is represented in the right panels.

At zero-magnetic field, the main effect of the temperature is to move the onset of hyperons to lower densities [41]. This feature is still true for a finite-magnetic field. However, the magnetic field affects the onset of the different hyperons: If no AMM is included, the onset of Σ^- is shifted to larger densities, the onset of Σ^+ is shifted to smaller densities, while the neutral

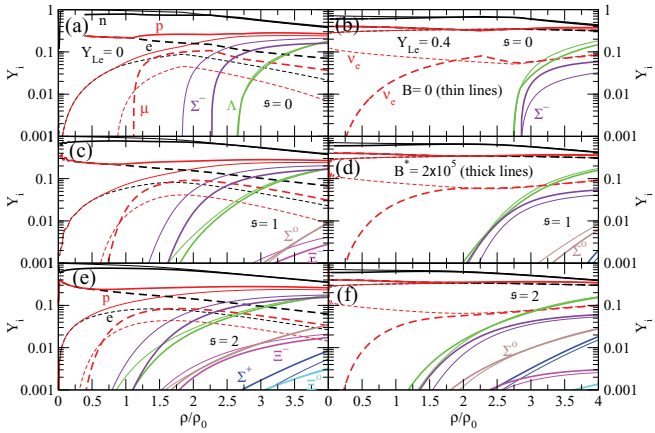

FIG. 4. (Color online) Particle fractions as a function of the baryonic density for $B^* = 0$ and 2×10^5 without AMMs for neutrino-free matter (left panel) and matter with trapped neutrinos (right panel) with $\mathfrak{s} = 0, 1, 2$.

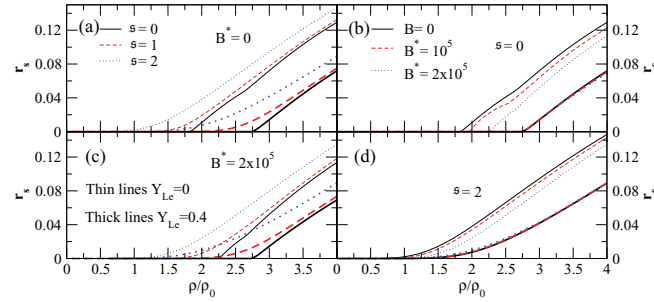

FIG. 5. (Color online) Strangeness fraction as a function of the baryonic density for several values of the magnetic field B and $\mathfrak{s} = 0, 1, 2$, without and with AMMs for the GM1 model. (Top panel) The strangeness fraction at a fixed entropy for different values of B, (bottom panel) the strangeness fraction at a fixed B for different values of the entropy per particle $\mathfrak{s}$.

hyperons are not much affected. In general, the onset of the negatively (positively) charged hyperons is shifted to larger (smaller) densities. If the AMM is included, the onset of the hyperons is defined not only by the charge, but also by the magnitude of the κ_b, and a more complex behavior is obtained.

As discussed in Refs. [19,49], the behavior observed among the different hyperons is mainly caused by a decrease in the neutron-chemical potential, because a smaller isospin asymmetry occurs, and a decrease in the electron-chemical potential caused by Landau quantization. In fact, at low densities, the fractions of proton and leptons are significantly affected by the magnetic field. The Landau quantization increases the proton abundance, and, therefore, the electron abundance because of the charge-neutrality condition. The inclusion of AMMs reduces the chemical potential of all the hyperons, and a complicated balance between the different terms, including the magnitude of the AMMs, defines whether the onset is shifted to larger or smaller densities. We have not shown the particle fractions with AMMs because the net effect of the onset of the different species of hyperons at different densities does not change the main properties of the star if magnetic fields below 10^{18} G are considered.

At $B = 0$ and $T = 0$, the presence of neutrinos shifts the onset of hyperons to larger densities because the neutron-chemical potential is smaller and the neutrino-chemical potential is finite. However, temperature makes this effect less effective. For warm matter under a strong magnetic field, we conclude that, if AMMs are not taken into account, a smaller chemical potential of both neutrons and neutrinos explains a smaller (larger) shift in the negatively (positively) charged hyperons to larger densities, and a smaller neutron-chemical potential gives rise to a shift to larger densities of the neutral hyperons onset, as compared to the neutrino-free case.

To summarize, we conclude that, in the presence of a strong magnetic field, we still have the onset of hyperons in warm stellar matter at lower densities as compared with cold matter at $B = 0$, however, according to the charge and flavor of the hyperon and the fraction of the leptons, the onset can occur at smaller or larger densities than the ones observed for $T = 0$ and $B = 0$.

The effect of the magnetic field on the total strangeness fraction is better seen in Fig. 5, where we show the total strangeness fraction for different values of a magnetic field at fixed entropy (right panel) and different values of the entropy per baryon $\mathfrak{s}$ at a fixed magnetic field (left panel). We only show results without AMMs. The fraction of the strangeness in the system is given by

$$r_{\mathfrak{s}} = \frac{\sum_b q_s^b \rho_b}{3\rho}, \tag{36}$$

where q_s^b is the strange charge of baryon b.

At zero entropy, the strangeness onset occurs below $2\rho_0$ and $3\rho_0$, respectively, for neutrino-free and neutrino-trapped matter, and at $\rho = 6\rho_0$, neutrino-trapped matter has a strangeness fraction 0.03–0.04 smaller than neutrino-free matter because of the larger electron fraction. In Figure 5, the left panel allows a comparison of the strangeness fraction at a fixed B and different entropies. As already pointed out, the temperature shifts the onset of strangeness to lower densities. Generally, this trend is still valid in the presence of a magnetic field for both neutrino-trapped and neutrino-free matter [48,50], except at large densities in neutrino-trapped matter, if the temperature is not high enough.

In the right panel of Fig. 5, we compare the strangeness fraction for fixed entropy per baryon and different magnetic-field intensities. The magnetic field lowers the strangeness fraction in neutrino-free matter, although at finite temperatures, this effect is smaller. On the other hand, the strangeness fraction in neutrino-trapped matter is almost not affected by the magnetic field. This behavior was already discussed in Ref. [49] and is explained by the presence of neutrinos. In neutrino-free matter, a smaller neutron fraction and the Landau quantization decrease the hyperon fraction. However, in matter with trapped neutrinos, the neutron-chemical potential does not suffer such a large reduction as in free-neutrino matter, and therefore, the strangeness fraction does not change much with the magnetic field, and it may even occur that the strangeness fraction increases with B at low density.

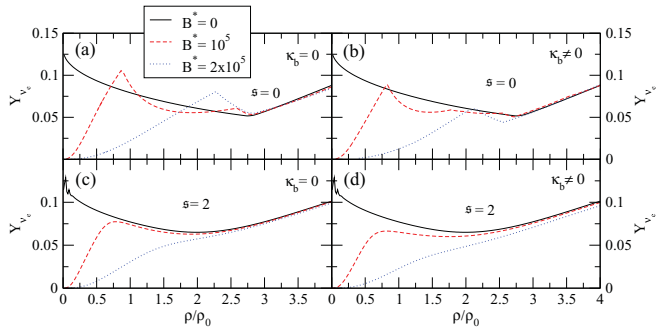

FIG. 6. (Color online) Neutrino fraction as a function of the baryonic density for several values of the magnetic field B and entropy per baryon $\mathfrak{s}$ without (left panel) and with (right panel) AMMs.

If the AMMs are included in the calculations, similar conclusions are obtained, and therefore, we do not show results with AMMs.

It is also interesting to analyze the effect of B on the neutrino fraction, which is shown in Fig. 6 as a function of the baryonic density for several values of a magnetic field and $\mathfrak{s} = 0, 2$. In Ref. [49], it was discussed that, for zero temperature, the magnetic field gave rise to a strong neutrino suppression at small densities as seen in the top panels. This was attributed to the large proton and, therefore, also attributed to electron fractions. At finite temperatures, the suppression at low densities persists, although the fluctuations caused by the filling of the LLs disappear. It is seen that, for a finite entropy also at high densities, a strong magnetic field gives rise to a decrease in neutrino fraction caused by the larger proton fraction that favors a larger electron fraction. A smaller neutrino fraction may imply a slower cooling of the star core, since the core essentially cools by neutrino emission [41]. The effect of AMMs is only noticeable at zero temperature.

In Fig. 7, the temperature of the system is plotted for an entropy per baryon $\mathfrak{s} = 1$ and 2, respectively, for neutrino-free

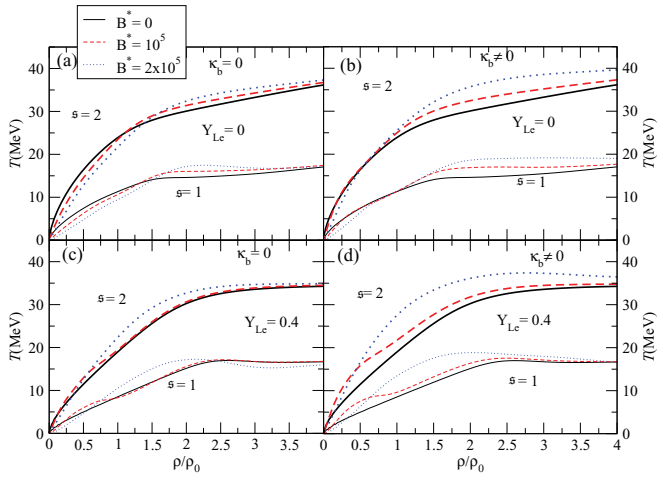

FIG. 7. (Color online) Temperature as a function of the baryonic density for several values of the magnetic field B without (left panels) and with (right panels) AMMs for neutrino-free matter (top panels) and matter with trapped neutrinos (bottom panels). The thin line is for $\mathfrak{s} = 1$, and the thick line is for $\mathfrak{s} = 2$.

matter and matter with trapped neutrinos. As expected, for a larger entropy per baryon, higher temperatures are reached. In a strong magnetic field, these temperatures can even be larger. At low densities, before the onset of hyperons, temperature rises slower for the larger magnetic fields because the proton (neutron) fraction increases (decreases) with B, and the nucleonic degrees of freedom become more equally distributed. The kink in all the curves identifies the onset of hyperons and, as discussed before, occurs at lower densities for lower values of B. This is true for both $\mathfrak{s} = 1$ and 2 with or without AMMs. At high densities, the temperature becomes approximately constant: This is clearly seen for $\mathfrak{s} = 1$; for $\mathfrak{s} = 2$, the temperature saturation occurs at higher densities because the hyperon fractions increase during a larger range of densities until they attain a saturation fraction. If AMMs are included, the temperature rises to larger values at finite B because of the larger lepton fraction and smaller hyperon fraction.

For matter with trapped neutrinos, we have a similar situation. However, because the proton fraction is larger, caused by the fixed lepton fraction constraint, the effect of B in reducing the neutron fraction at low densities is not so large, and the differences in the dependence of T on the baryonic density below $2\rho_0$ is mainly defined by the neutrino fraction. Also, a smaller overall neutron fraction favors lower temperatures as compared with neutrino-free matter.

We finish the discussion on the effect of the magnetic field on warm stellar matter by summarizing the main conclusions: (a) All the effects of the magnetic field discussed at zero temperature are still valid but are diluted partially because of the partial filling of the different LL levels for charged particles or spin levels for particles with an AMM; (b) Landau quantization softens the EOS and makes stellar matter less isospin asymmetric, therefore, matter with trapped neutrinos will never be softer than neutrino-free matter even before the hyperon onset; (c) just as for $B = 0$, for a fixed magnetic field, increasing the temperature increases the strangeness fraction, however, the overall strangeness fraction in the star is smaller for a larger magnetic field; (d) there is a neutrino suppression at low densities and an overall smaller neutrino fraction in a protoneutron star with a strong magnetic field, which implies a slower cooling process; (e) at low densities, temperature increases slower with density at fixed entropy for the stronger magnetic fields because of the smaller asymmetry of stellar matter; at high densities, larger temperatures are attained because of a larger electron fraction and a smaller negatively charged hyperon fraction.

In the following, we study the properties of protoneutron stars with strong magnetic fields. Since to date, there is no information available on the interior magnetic field of the star, we assume that the magnetic field is baryon-density dependent as suggested by Ref. [13]. The variation in magnetic field B with baryon density ρ from the center to the surface of a star is parametrized [13,14] by the following form:

$$B\left(\frac{\rho}{\rho_0}\right) = B^{\rm surf} + B_0\left[1 - \exp\left\{-\beta\left(\frac{\rho}{\rho_0}\right)^{\gamma}\right\}\right], \quad (37)$$

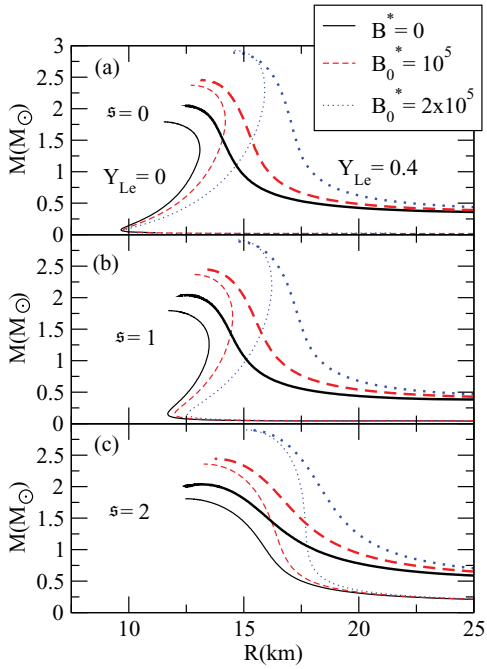

FIG. 8. (Color online) Mass-radius curve of neutron stars for several values of the magnetic field by using a density-dependent magnetic field B given by Eq. (37). Thin lines correspond to neutrino-free matter, and thick lines correspond to trapped neutrino matter with lepton fraction $Y_{\rm Le} = 0.4$.

where ρ_0 is the saturation density, $B^{\rm surf}$ is the magnetic field at the surface taken equal to 10^{15} G in accordance with the values inferred from observations, and B_0 represents the magnetic field at large densities. The parameters β and γ are chosen in such a way that the field decreases with the density from the center to the surface. In this paper, we use the set of values $\beta = 0.05$ and $\gamma = 2$ to allow a slowly varying field with the density. The magnetic field will be considered in units of the critical field $B_e^c = 4.414 \times 10^{13}$ G so that $B_0 = B_0^* B_e^c$. We take B_0^* as a free parameter to check the effect of magnetic fields on stellar matter. Here, we consider the EOS by taking the hyperon-meson-coupling constants $x_\sigma = 0.6$.

Hadron-star properties are obtained from the EOS studied, for several values of magnetic field, by solving the Tolman-Oppenheimer-Volkoff equations, which result from the Einstein general relativity equations for spherically symmetric static stars. This is an approximation since the magnetic field destroys the spherical symmetry, and therefore, we interpret the obtained results as average values. We do not allow the magnetic field at the center of the star to exceed $\sim 3 \times 10^{18}$ G according to the results of Ref. [19], which indicate that stable stars do not occur with a larger central magnetic field.

In Fig. 8, we show the family of stars, which correspond to the maximum mass configuration given in Tables II and III. Two main conclusions may be drawn: (a) warm stars with trapped neutrinos have larger masses and radii. However, the differences get smaller for the most massive stars if a strong magnetic field exists; (b) a strong magnetic field makes the star radius and the mass of the maximum mass star configuration larger.

In Table II, the maximum gravitational and baryonic masses of stable stars, their radii, central energy densities, and magnetic fields at the center are given for neutrino-free matter. In Table III, the same quantities are displayed for matter with trapped neutrinos.

The main conclusions we draw from the tables are as follows: (a) for a finite-magnetic field and neutrino-free stars, the maximum gravitational mass decreases slightly with $\mathfrak{s}$, however, the opposite occurs for $B = 0$; (b) for stars with trapped neutrinos, the maximum baryonic mass of the star generally decreases with an increase in $\mathfrak{s}$, (c) in the presence of large magnetic fields, the central baryonic density of the star decreases with an increase in B and/or temperature. On the other hand, both B and T increase the star radius, (d) the strength of the magnetic field increases from 10^{15} G at the surface to a maximum of $\sim 3 \times 10^{18}$ G at the center.

Neutrinos diffuse out of the core after a first period when they are trapped in the core of a protoneutron and the star reaches an entropy per particle of $\mathfrak{s} \sim 1$ (in units of the Boltzmann constant). During the deleptonization period, the core is heated up and reaches an entropy per particle of $\mathfrak{s} \sim 2$. After the core deleptonizes, exotic degrees of freedoms, such as hyperons will appear. We will discuss how the magnetic field may influence the evolution of the star from a stage with $\mathfrak{s} = 1$ and trapped neutrinos to a stage of warm neutrino-free matter with $\mathfrak{s} = 2$ and finally, a cold neutrino-free star with

TABLE II. Properties of the stable baryon star with maximum mass for several values of a magnetic field using [see Eq. (37)] the parametrization. $M_{\rm max}$, $M^b_{\rm max}$, R, E_0, ρ^c, B_c, and T_c, respectively, are the gravitational and baryonic masses, the star radius, the central energy density, the central baryonic density, and the values of the magnetic field and the temperature at the center. Neutrino-free matter.

B_0^*	$\mathfrak{s}$	$M_{\rm max}$ ($M_\odot$)	$M^b_{\rm max}$ [($\odot$)	R (km)	E_0 (fm^{-4})	ρ_c (fm^{-3})	B_c (G)	T_c (MeV)
$B = 0$	0	1.790	2.033	11.527	5.939	0.985		
	1	1.794	2.024	11.717	5.854	0.967		19.24
	2	1.808	2.004	12.467	5.656	0.922		40.79
$B_0^* = 10^5$	0	2.372	2.672	12.694	4.846	0.688	2.812×10^{18}	
	1	2.368	2.652	12.796	4.860	0.687	2.808×10^{18}	17.96
	2	2.358	2.597	13.269	4.837	0.674	2.746×10^{18}	37.43
$B_0^* = 2 \times 10^5$	0	2.926	3.234	14.509	3.629	0.454	3.150×10^{18}	
	1	2.919	3.207	14.630	3.616	0.451	3.117×10^{18}	15.92
	2	2.902	3.147	15.032	3.612	0.445	3.040×10^{18}	33.54

TABLE III. Properties of the stable baryon star with maximum mass for several values of a magnetic field by using [see Eq. (37)] the parametrization. $M_{\rm max}$, $M^b_{\rm max}$, R, E_0, ρ^c, B_c, and T_c, respectively, are the gravitational and baryonic masses, the star radius, the central energy density, the central baryonic density, and the values of the magnetic field and the temperature at the center. Neutrino-trapped matter.

B_0^*	$\mathfrak{s}$	$M_{\rm max}$ ($M_\odot$)	$M^b_{\rm max}$ ($M_\odot$)	R (km)	E_0 (fm^{-4})	ρ_c (fm^{-3})	B_c (G)	T_c (MeV)
$B=0$	0	2.046	2.293	12.455	5.420	0.856		-
	1	2.040	2.271	12.529	5.395	0.847		16.21
	2	2.036	2.226	13.198	5.192	0.808		34.78
$B_0^*=10^5$	0	2.454	2.694	13.123	4.819	0.660	2.678×10^{18}	
	1	2.449	2.686	13.122	4.842	0.662	2.682×10^{18}	16.76
	2	2.441	2.641	13.622	4.731	0.644	2.593×10^{18}	34.72
$B_0^*=2\times10^5$	0	2.889	3.063	14.547	3.886	0.464	3.261×10^{18}	
	1	2.890	3.071	14.621	3.834	0.461	3.228×10^{18}	16.81
	2	2.897	3.058	15.094	3.720	0.451	3.117×10^{18}	33.83

$\mathfrak{s}=0$. During this evolution, the gravitational mass of the star decreases, but its baryonic mass stays constant.

At zero-magnetic field, the maximum baryonic mass of a star with trapped neutrinos and $\mathfrak{s}=1$ is 2.27 $M_\odot$. This star will deleptonize and will heat up. However, since the maximum baryonic mass of a neutrino-free star with $\mathfrak{s}=2$ is 0.27 $M_\odot$ smaller (equal to 2.00 $M_\odot$), the star will evolve into a low-mass black hole [41]. This is caused by the softening that the EOS suffers with the appearance of hyperons and is well illustrated in Fig. 9 by the full lines: For $B=0$, all configurations with trapped neutrinos and a baryonic mass above the maximum of the neutrino-free $\mathfrak{s}=2$ configurations 2.024 $M_\odot$ will evolve into a black hole.

We will now consider that the decay of the magnetic field will occur in a much longer time scale than the deleptonization phase, and therefore, during the star evolution, the magnetic field will remain constant. If we consider $B_0^*=10^5$, the maximum baryonic mass of a star with trapped neutrinos and $\mathfrak{s}=1$ is 2.69 $M_\odot$. The maximum mass of a neutrino-free star with $\mathfrak{s}=2$ is smaller, but the difference is much smaller than the one, which occurs at $B=0$: A maximum mass of 2.60 $M_\odot$ only corresponds to a 0.09-$M_\odot$ difference. The set of stars that will evolve into a low-mass black hole will be much smaller. In Fig. 9, the dashed curves correspond to $B_0^*=10^5$, from top to bottom, $\mathfrak{s}=1$ with trapped neutrinos, neutrino-free $\mathfrak{s}=2$ and $\mathfrak{s}=0$. The configurations of a star with trapped neutrinos and $\mathfrak{s}=1$ above the maximum of the neutrino-free $\mathfrak{s}=2$ curve 2.597 $M_\odot$ will evolve into a black hole. However, if we consider $B_0^*=2\times10^5$, all configurations with trapped neutrinos and $\mathfrak{s}=1$ will evolve into stable $\mathfrak{s}=2$ and afterward, into $\mathfrak{s}=0$ neutrino-free star configurations. The maximum mass star configuration with trapped neutrinos and $\mathfrak{s}=1$ is smaller than the maximum mass neutrino-free star with $\mathfrak{s}=2$, 3.07 $M_\odot$ and 3.15 $M_\odot$, respectively. No evolution into a low-mass black hole will occur. This could be expected, since we have discussed that the magnetic field hinders the appearance of hyperons.

However, it is important to notice that, if the star cools down into a stable star, which keeps the magnetic-field configuration described by Eq. (37) with $B_0^*=2\times10^5$, it may still decay into a low-mass black hole during the magnetic-field decay.

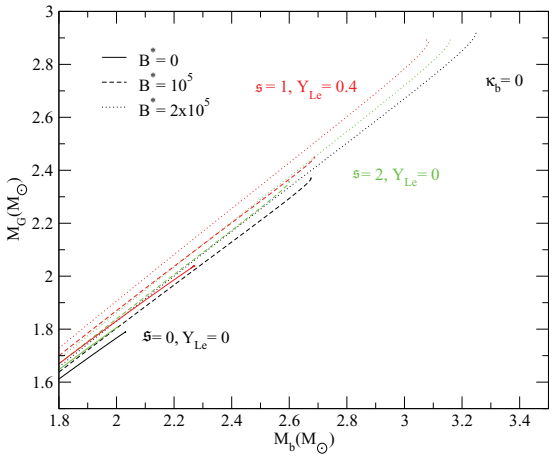

FIG. 9. (Color online) Gravitational mass as a function of the baryonic mass of neutron stars for several values of the magnetic field by using a density-dependent magnetic field B given by Eq. (37).

IV. CONCLUSIONS

In the present paper, we have studied the effect of a very strong magnetic field on the EOS and properties of warm stars. We have used a relativistic mean-field model with the GM1 parameter set [43] and have considered stellar matter both neutrino free and with trapped neutrinos.

All the effects of the magnetic field discussed at zero temperature are still valid: In neutrino-free matter, the EOS becomes softer at low densities because of the Landau quantization suffered by protons and becomes harder at large densities because the onset of hyperons is shifted to larger densities; in matter with trapped neutrinos, spin polarization of neutrons contributes to a larger neutron degeneracy pressure and hardens the EOS. However, these effects are partially diluted because of the partial nonzero filling of the different LLs for charged particles or spin levels for particles with an AMM at finite temperatures.

Just as for $B=0$, for a fixed magnetic field, to increase the temperature increases the strangeness fraction. However, the

overall strangeness fraction in the star is smaller for a larger magnetic field. In matter with trapped neutrinos, the opposite may occur, and for $\mathfrak{s} = 2$, the larger the magnetic field, the larger the strangeness fraction below $\rho = 3\rho_0$.

Previously, it was shown that there was a strong neutrino suppression at low densities for finite-magnetic fields [49]. For a finite entropy also at high densities, a strong magnetic field gives rise to a decrease in the neutrino fraction caused by the larger proton fraction that favors a larger electron fraction. A smaller neutrino fraction may imply a slower cooling of the star core, since the core essentially cools by neutrino emission [41].

It has been shown that a strong magnetic field increases the mass and radius of the most massive cold stable star configuration [19]. This is still true for warm stars. The radius of these stars increases with $\mathfrak{s}$, just as it occurs for $B = 0$ [41,47] but at a much smaller rate. On the other hand, their baryonic masses decrease with the entropy per particle, and the larger decrease occurs for the larger magnetic field. For stronger magnetic fields, the contribution of the magnetic field to the total EOS is larger, which gives rise to a stiffer EOS. As a result, the star central energy density and baryon density decrease as the magnetic field increases.

The mass of the observed neutron stars may set an upper limit on the possible magnetic field acceptable in the interior of a star. Of course, it may also occur that the most massive stars decay into low-mass black holes when the magnetic field in their interior decays.

For $B = 0$, a hybrid star may evolve into a low-mass black hole because the maximum baryonic mass of a warm star with trapped neutrinos and an entropy per particle $\mathfrak{s} \sim 1$ is larger than the maximum mass of a warm deleptonized star with $\mathfrak{s} = 2$ or a cold deleptonized star [41,50]. In the present paper, it was shown that, for a strong enough magnetic field, the star would cool down as a stable compact star, if the magnetic field did not decay during the deleptonization phase. However, the decay of the magnetic field may cause star instability and, consequently, the formation of a black hole.

ACKNOWLEDGMENTS

This work was partially supported by FCT/FEDER under Project Nos. PTDC/FIS/113292/2009 and CERN/FP/116366/2010, and by COMPSTAR, an ESF Research Networking Programme.

[1] R. C. Duncan and C. Thompson, Astronphys. J. **392**, L9 (1992).
[2] V. V. Usov, Nature (London) **357**, 472 (1992).
[3] B. Paczyński, Acta Astronaut. **42**, 145 (1992).
[4] C. Kouvellioton, Nature (London) **393**, 235 (1998).
[5] K. Hurley *et al.*, Astrophys. J. **510**, L111 (1999).
[6] S. Mareghetti and L. Stella, Astrophys. J. **442**, L17 (1995); J. vanParadijs, *ibid.* **513**, 464 (1999).
[7] S. L. Shapiro and S. A. Teukolsky, *Black Holes, White Dwarfs and Neutron Stars* (Wiley Interscience, New York, 1983).
[8] L. Ferrario and D. Wickrammasinghe, Mon. Not. R. Astron. Soc. **367**, 1323 (2006).
[9] A. Iwazaki, Phys. Rev. D **72**, 114003 (2005).
[10] J. Vink and L. Kuiper, Mon. Not. R. Astron. Soc.: Letters **370**, L14 (2006).
[11] A. Broderick, M. Prakash, and J. M. Lattimer, Astrophys. J. **537**, 351 (2000).
[12] C. Y. Cardall, M. Prakash, and J. M. Lattimer, Astrophys. J. **554**, 322 (2001).
[13] D. Bandyopadhyay, S. Chakrabarty, and S. Pal, Phys. Rev. Lett. **79**, 2176 (1997); S. Chakrabarty, Phys. Rev. D **54**, 1306 (1996).
[14] G.-J. Mao, A. Iwamoto, and Z.-X. Li, Chin. J. Astron. Astrophys. **3**, 359 (2003).
[15] F. X. Wei, G. J. Mao, C. M. Ko, L. S. Kisslinger, H. Stöcker, and W. Greiner, J. Phys. G **32**, 47 (2006).
[16] A. Pérez-Martínez, H. Pérez-Rojas, and H. J. Mosquera-Cuesta, Eur. Phys. J. C **29**, 111 (2003).
[17] P. Yue and H. Shen, Phys. Rev. C **74**, 045807 (2006).
[18] A. Rabhi, C. Providência, and J. Da Providência, J. Phys. G **35**, 125201 (2008).
[19] A. Broderick, M. Prakash, and J. M. Lattimer, Phys. Lett. B **531**, 167 (2002).
[20] P. Dey, A. Bhattacharyya, and D. Bandyopadhyay, J. Phys. G **28**, 2179 (2002).
[21] I.-S. Suh and G. J. Mathews, Astrophys. J. **546**, 1126 (2001).
[22] K. Takahashi, J. Phys. G **34**, 653 (2007).
[23] P. Yue and H. Shen, Phys. Rev. C **77**, 045804 (2008).
[24] P. Yue, F. Yang, and H. Shen, Phys. Rev. C **79**, 025803 (2009).
[25] A. Rabhi, H. Pais, P. K. Panda, and C. Providência, J. Phys. G **36**, 115204 (2009).
[26] D. Bandopadhyay, S. Pal, and S. Chakrabarty, J. Phys. G **24**, 1647 (1998); S. Pal, D. Bandopadhyay, and S. Chakrabarty, *ibid.* **25**, L117 (1999).
[27] H. Pais, M.S. thesis, University of Coimbra, 2008.
[28] D. P. Menezes, M. Benghi Pinto, S. S. Avancini, A. Pérez Martínez, and C. Providência, Phys. Rev. C **79**, 035807 (2009).
[29] D. Ebert and K. G. Klimenko, Nucl. Phys. A **728**, 203 (2003).
[30] R. González Felipe, A. Pérez Martínez, H. Pérez Rojas, and M. Orsaria, Phys. Rev. C **77**, 015807 (2008).
[31] D. P. Menezes, M. Benghi Pinto, S. S. Avancini, and C. Providência, Phys. Rev. C **80**, 065805 (2009).
[32] A. Júlia Mizher, M. N. Chernodub, and E. S. Fraga, Phys. Rev. D **82**, 105016 (2010).
[33] E. J. Ferrer, V. de la Incera, J. P. Keith, I. Portillo, and P. L. Springsteen, Phys. Rev. C **82**, 065802 (2010).
[34] A. Rabhi and C. Providência, Phys. Rev. C **83**, 055801 (2011).
[35] E. J. Ferrer, V. de la Incera, and C. Manuel, Phys. Rev. Lett. **95**, 152002 (2005); Nucl. Phys. B **747**, 88 (2006).
[36] E. J. Ferrer and V. de la Incera, Phys. Rev. Lett. **97**, 122301 (2006); Phys. Rev. D **76**, 045011 (2007); **76**, 114012 (2007).
[37] J. L. Noronha and I. A. Shovkovy, Phys. Rev. D **76**, 105030 (2007).
[38] K. Fukushima and H. J. Warringa, Phys. Rev. Lett. **100**, 032007 (2008).
[39] L. Paulucci, E. J. Ferrer, V. de la Incera, and J. E. Horvath, Phys. Rev. D **83**, 043009 (2011).
[40] R. González Felipe, D. Manreza Paret, and A. Pérez Martinez, Eur. Phys. J. A **47**, 1 (2011).
[41] M. Prakash, I. Bombaci, M. Prakash, P. J. Ellis, J. M. Lattimer, and R. Knorren, Phys. Rep. **280**, 1 (1997)

[42] B. D. Serot and J. D. Walecka, Adv. Nucl. Phys. **16**, 1 (1986); J. Boguta and A. R. Bodmer, Nucl. Phys. A **292**, 413 (1977).
[43] N. K. Glendenning and S. A. Moszkowski, Phys. Rev. Lett. **67**, 2414 (1991).
[44] N. K. Glendenning, *Compact Stars* (Springer-Verlag, New York, 2000).
[45] A. Burrows and J. M. Lattimer, Astrophys. J. **307**, 178 (1986).
[46] M. Chiapparini, M. E. Bracco, A. Delfino, M. Malheiro, D. P. Menezes, and C. Providência, Nucl. Phys. A **826**, 178 (2009).
[47] D. P. Menezes and C. Providência, Phys. Rev. C **68**, 035804 (2003).
[48] P. K. Panda, C. Providência, and D. P. Menezes, Phys. Rev. C **82**, 045801 (2010).
[49] A. Rabhi and C. Providência, J. Phys. G **37**, 075102 (2010).
[50] D. P. Menezes and C. Providência, Phys. Rev. C **69**, 045801 (2004).